A Method to Extract Various Vascular Features from Liver Images of Computed Tomography

M. Ishikawa[14], H. Uchida[1], T. Tamaki[1], M. Yamamoto[24], T. Suda[3], M. Igarashi[3], Y. Aoyagi[3]
[1]Graduate School of Science and Technology, Niigata University, Niigata, Japan
[2]Faculty of Engineering, Niigata University, Niigata, Japan
[3]Institute of Medicine Density, Academic Assembly, Niigata University, Niigata, Japan
[4]The Center for Transdisciplinary Research, Niigata University, Niigata, Japan

Abstract –**Liver cirrhosis is a diagnosis based on histological concept. However, liver biopsy, sampling liver tissues from a living donor, is an invasive technique, in which a direct puncture of the liver is necessary. On the other hand, a higher resolution of a recent computed tomography has a potential to replace histology with objective and digital images, which are available without any invasive techniques. Here we present a system extracting various features of three-dimensional vasculature in the liver from images of CT aiming an objective and noninvasive diagnosis of liver cirrhosis.**

Keywords – **Computer aided diagnosis, Liver cirrhosis, Computed Tomography.**

I. Introduction

Although rapid improvements of imaging modalities in medical fields have been achieved, demanding of structural evaluation to grade chronic liver disease forces sampling of liver tissues using a risky procedure, liver biopsy, still now. In general histological disorganization of the liver is easily recognized as an irregular reconstruction of normal vasculature [1]. However, histological evaluation is neither digital nor objective rather descriptive.

Alternative diagnosis might be achieved using images with Computed Tomography (CT). There are some ways to image a liver using CT; CT during arterial portography (CTAP), CT during hepatic arteriography (CTHA), and intravenous dynamic contrast enhanced CT. These methods are safer and less invasive than the biopsy. But, a diagnosis using CT-images by a doctor is based on doctor's skill and experience, and is subjective rather than objective.

Therefore, many researchers have been developed a computer-aided diagnostic method during recent two decades using digital images including CT images of liver such as a method for extracting a region of a liver from CT-images, and detecting blood vessels in a liver[2]. But most of these conventional methods are aimed to diagnosis liver cancer not hepatic cirrhosis, which is one of most terrible liver diseases.

In this paper we propose a method to extract various vascular features from liver images of CT for diagnosis of hepatic cirrhosis. This method extracts three-dimensional shape of blood vessels in the liver from CT-images, and analyzes the topology of vascular shape.

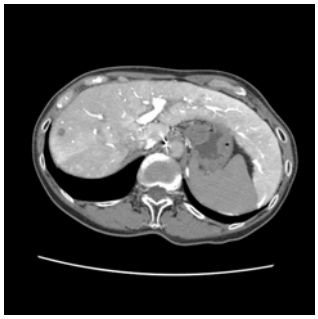

Figure.1-CTAP

Figure.2-DynamicCT

II. Materials

We use 72 CT-images (1.0mm/pixel) in 5.0mm thickness from CTAP performed with an injection of 95ml of non-ionic contrast agent at a concentration of 150mg I/ml through a catheter placed in the superior mesenteric artery[3]. Each image is converted from 16 bits to 8 bits by AccuLite 3D WorkStation (AccuImage Diagnostics Corporation).

III. Extracton of the blood vessels

This section describes extraction of blood vessels from each image, and three dimensional labeling and thinning of extracted vessels.

First, each image is binarized with a threshold to extract regions of blood vessels (portal veins in this case) in the liver. Vessels are imaged angiographically in white so that they are discriminated from surrounding liver tissues.

Threshold value is locally determined in order to remove small white regions, which are not corresponding to blood vessels in the liver. The image is divided into small rectangle regions in 5x5 size, and a threshold value are determined for each region. Let (x, y) denote a pixel in the small region in the original image, $E(x, y) \in [0,255]$ denote the intensity of pixel (x, y), and $E_b(x, y)$ denote an edge intensity that is obtained with the prewitt filter and is binarized with an appropriate threshold:

$$E_b(x, y) = \begin{cases} 1, & E_b(x, y) >= 80 \\ 0, & \text{Otherwise} \end{cases}, \qquad (1)$$

and a set of edge pixels EB is defined as following:

$$EB \equiv \{(x,y) \mid E_b(x,y) = 1\}. \quad (2)$$

Next, histogram H of EB is made as following:

$$EB[i] = \{(x,y) \mid (x,y) \in EB \wedge E(x,y) = i\},$$
$$H[i] = \mid EB[i] \mid, \quad (3)$$

where i denotes the index of bins (intensity) for the histogram. Here S and S' are defined as:

$$S = \sum_{i=0}^{255} H[i], \quad (4)$$

$$S' = \sum_{i=0}^{Th} H[i]. \quad (5)$$

Th is the threshold and is defined as the smallest value satisfying the following equation:

$$\frac{S'}{S} \geq 0.95 \quad (6)$$

Fig.3 shows the relation among S, S' and Th. Furthermore, the final binary image is obtained by taking logical product of the edge-based binary image locally thresholded in each small region with Th and a globally thresholded image with some threshold.

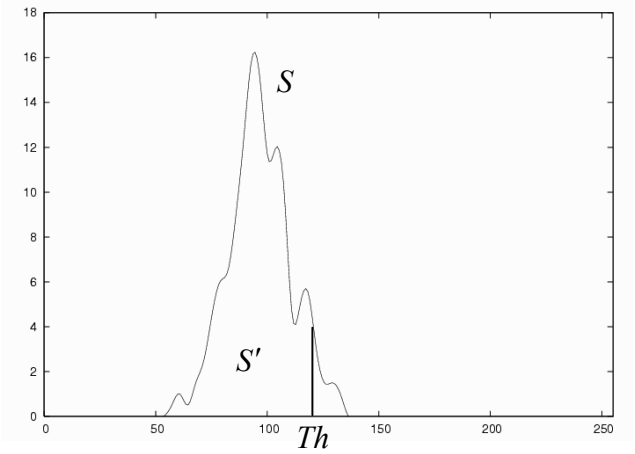

Figure.3-decision threshold

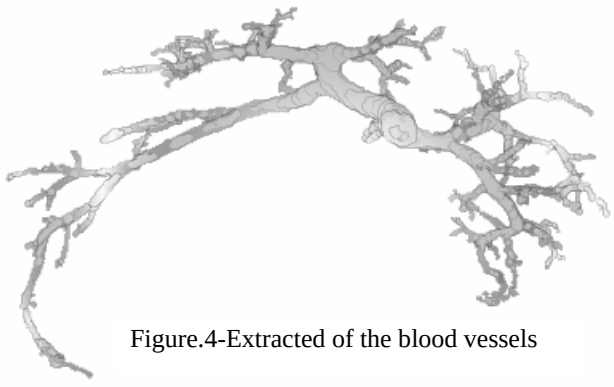
Figure.4-Extracted of the blood vessels

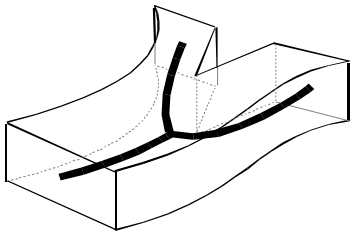
Figure.5-Example of the thinning

Next, a three-dimensional labeling process in 26 neighbors is applied on the binarized consecutive 72 CT-images to separate volumetric regions into the backbone, ribs, blood vessels and internal organs. Among labeled regions, the third largest region is determined as the region of blood vessels because the first and second largest regions correspond to the bone and a plate for radiography existing outside of the body, respectively. Figure 4 shows a rendered image of three-dimensionally reconstructed blood vessels in the liver. Visualization was performed by using the VOLUME-ONE software provided by the VOLUME-ONE developer group and available on the Internet (http://www.volume-one.org). Note that the intestines are removed by hand.

Thinning process is an endpoint to see the topology of blood vessels such as endpoint and branches. Thinning process changes from volumetric shapes to line shapes (Figure 5) [4][5][6]. In this research Euclid distance transform for thinning process is used because it is not influenced by rotation of shape and it does not generate a fake branch that has a bad effect upon successive procedures. Figure 6 shows thinned blood vessels. We extract vascular features from the thinning line shape and the volumetric shape (not thinned).

In next two sections, knowledge of vasculature of hepatic cirrhosis and definitions of features are described.

IV. ASSUMPTION

To detect the progression of chronic liver diseases, we focus only on the vasculature (geometry of blood vessels) in

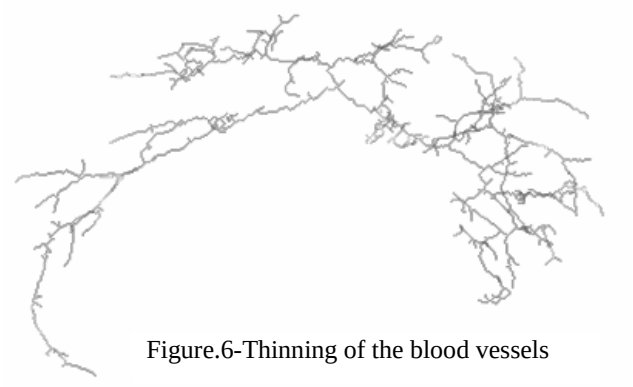
Figure.6-Thinning of the blood vessels

the liver. We made the following four assumptions on the vasculature, and each descriptive and qualitative assumption shows the difference of among normal and cirrhotic livers.

1. Deformation of the blood vessels in the liver

In normal liver hepatocytes form regular hexagonal structure and a smooth vascular network surrounds entire hepatocytes to ensure sufficient blood supply in each hepatocytes. As disease progression from chronic hepatitis to liver cirrhosis, continuous degeneration and regeneration of hepatocytes lead to destruction of regular hexagonal conformation and deformation of vasculature between branch points of vessels. In normal liver the right lobe is significantly larger than the left one. As the progress of liver disease, degeneration and regeneration of the liver take place not evenly in each lobe; continuous atrophy of the right lobe followed by a decompensating enlargement of the left one.

2. Change of branch angles

Generally vessels branch like a tree in the liver. Regular branching angles in normal liver deviates along the course of disease progression.

3. Fractality changes

Blood vessels in brain, lung and liver have fractal shapes. The progress of liver diseases alters or the fractality and fractal dimension of the vasculature in the liver [7].

V. Extraction of the Features

According to the assumptions in the previous section, we define four features of the vasculature that represent the progress of liver cirrhosis.

Here we describe several definitions related to the features (see Figure 7). A branch point (or junction point) $\mathbf{c}^j$ is *j*-th branch of a blood vessel, and connects to a single voxel of a line shape in 26 neighbors. An endpoint is a leaf node of a tree structure of blood vessels, and connects to at least three voxels in 26 neighbors. A segment $\mathbf{b}^i$ represents *i*-th blood vessel between branch points, and is comprised of N_i voxels. $\mathbf{b}_n^i$ represents a three dimensional vector of *n*-th voxel composing the segment $\mathbf{b}^i$.

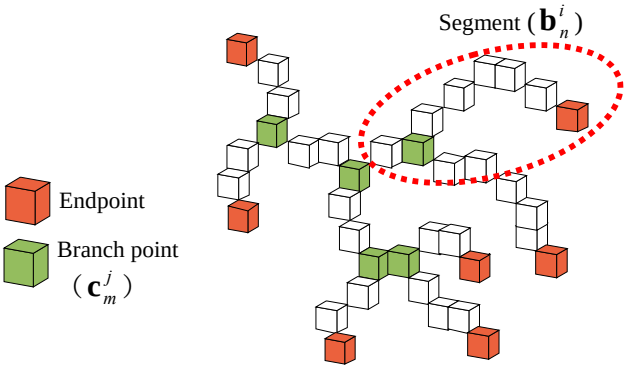

Figure.7-Branch point and Segment

Features in section 6.1, 6.2, 6.3 and 6.4 use the thinning line shape, while a feature in section 6.5 uses the volumetric shape (not thinned) of blood vessels.

6.1 Ratio of segment length and distance between branches

This feature is represented by a ratio of length of a segment and distance between branches connected to the segment. Each segment is numbered as $\mathbf{b}^i$ so that the first segment $\mathbf{b}^1$ is the portal vein entered into the liver. Then the length l^i of a segment $\mathbf{b}^i$ is defined as the sum of Euclid distances between adjacent voxels in the segment:

$$l_i = \sum_{n=1}^{N_i-1} \left| \mathbf{b}_n^i - \mathbf{b}_{n+1}^i \right|, \tag{7}$$

and the distance between two branch points is defined as following:

$$a_i = \left| \mathbf{b}_1^i - \mathbf{b}_N^i \right|, \tag{8}$$

where the distance of a segment comprised of a single voxel defined as 0. The ratio between l^i and a_i is defined as following:

$$r_i = \frac{l_i}{a_i}. \tag{9}$$

6.2 Curvature of segment

This feature is represented by three-dimensional k-curvature of a segment. Three dimensional curvature $\phi\left(\mathbf{b}_n^i\right)$ at $\mathbf{b}_n^i$ is given by angle change of tangent vector. Actually the curvature in digital line shape is calculated with the distance between two voxels at k distance. The tangent vector $\mathbf{t}_n^i$ is defined as following:

$$\mathbf{t}_n^i = \mathbf{b}_{n+k}^i - \mathbf{b}_n^i \tag{10}$$

Angle change of tangent vector ϕ_n^i at each voxel is defined as following (see Figure 8):

$$\phi_n^i = \cos^{-1} \frac{\mathbf{t}_{n+1}^i \cdot \mathbf{t}_n^i}{\left|\mathbf{t}_n^i\right|\left|\mathbf{t}_n^i\right|} \tag{11}$$

Therefore, ϕ^i for i-th segment is defined as following:

$$\phi^i = \sum_{n=1}^{N} \phi_n^i \tag{12}$$

6.3 Torsion of segment

This feature is represented by torsion to line shape of target. Torsion is given by angle change of binormal vector. Binormal vector $\mathbf{d}_n^i$ is defined as following:

$$\mathbf{d}_n^i = \mathbf{t}_n^i \times \mathbf{t}_{n+1}^i . \tag{13}$$

Torsion φ_n^i is defined as following (see Figure 9):

$$\varphi_n^i = \cos^{-1} \frac{\mathbf{d}_{n+1}^i \cdot \mathbf{d}}{\left|\mathbf{d}_{n+1}^i\right|\left|\mathbf{d}\right|} . \tag{14}$$

Therefore, torsion of each segment is defined as following:

$$\varphi_i = \sum_{n=1}^{N} \varphi_n^i . \tag{15}$$

6.4 Branch angle

This feature is represented by angle of branch. Branch angle is given by center points $\mathbf{b}_1^c, \mathbf{b}_2^c$ of two segments and a branch point $\mathbf{c}^c$ (see Figure 10). The angle θ of a branch point is defined as following:

$$\theta = \cos^{-1}\left(\frac{\left(\mathbf{b}_1^c - \mathbf{c}^c\right) \cdot \left(\mathbf{b}_2^c - \mathbf{c}^c\right)}{\left|\mathbf{b}_1^c - \mathbf{c}^c\right|\left|\mathbf{b}_2^c - \mathbf{c}^c\right|} \right) . \tag{16}$$

VI. Result and Discussion

We have implemented the proposed features of the vasculature defined in the previous section, and conducted an experiments for CTAP images (see Section II) of three subjects I, T and S of liver cirrhosis (note that the subject T is better than the others). Results of the features calculated for each subject are shown in Figure 11. Each plot in Fig. 11 is a histogram of the feature calculated for the right and left hepatic lobe respectively, normalized from 0 to 1 by dividing by the total amount of the feature.

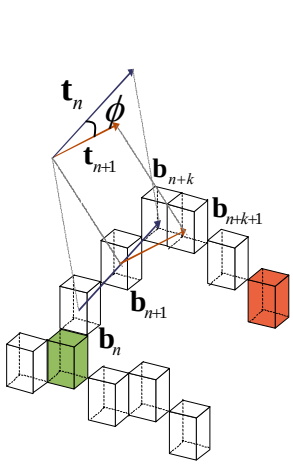

Figure.8-Curvature of vessels

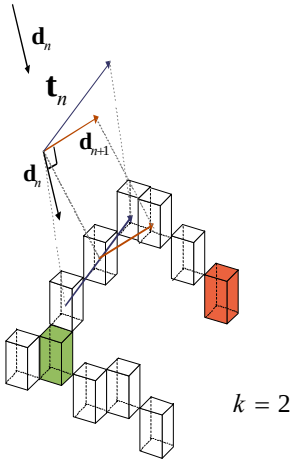

Figure.9-Torsion of vessels

The branch angles of the left lobe of subject I has a distribution with a broad peak centered around 100 degrees, and that of the right lobe has no significant distribution. For subject T, the branch angles have a peak around 100 degrees for both the right and left lobes, and for the left lobe of subject S has a similar distribution. The angles for the right lobe of subject S has no remarkable peaks in the distribution that is relatively similar to that of subject I than that of subject T. Note that the peaks at 10 degrees for subject I and T are not meaningful because of the incompleteness of the feature calculation.

In the distributions of the curvature for subject I and S, large peaks between 0.3 and 0.5 can be seen. That for subject T is also similar except the peak for the left lobe is larger than that for the right lobe and an additional peak exists around 1.1.

The distributions of torsion are the same distribution with a broad peak around 0.4 for all subjects, but in the right lobe of subject I there is a prominent peak at 0.2. It is not reliable because the number of torsions that could be calculated is very small (only 15 torsions). The distributions of the ratio are all similar shapes with a peak around 0.3.

We can see the differences between the distributions of

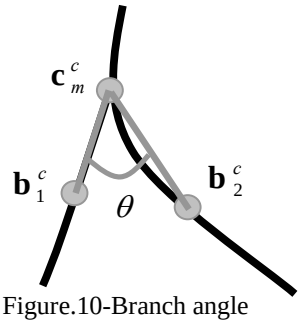

Figure.10-Branch angle

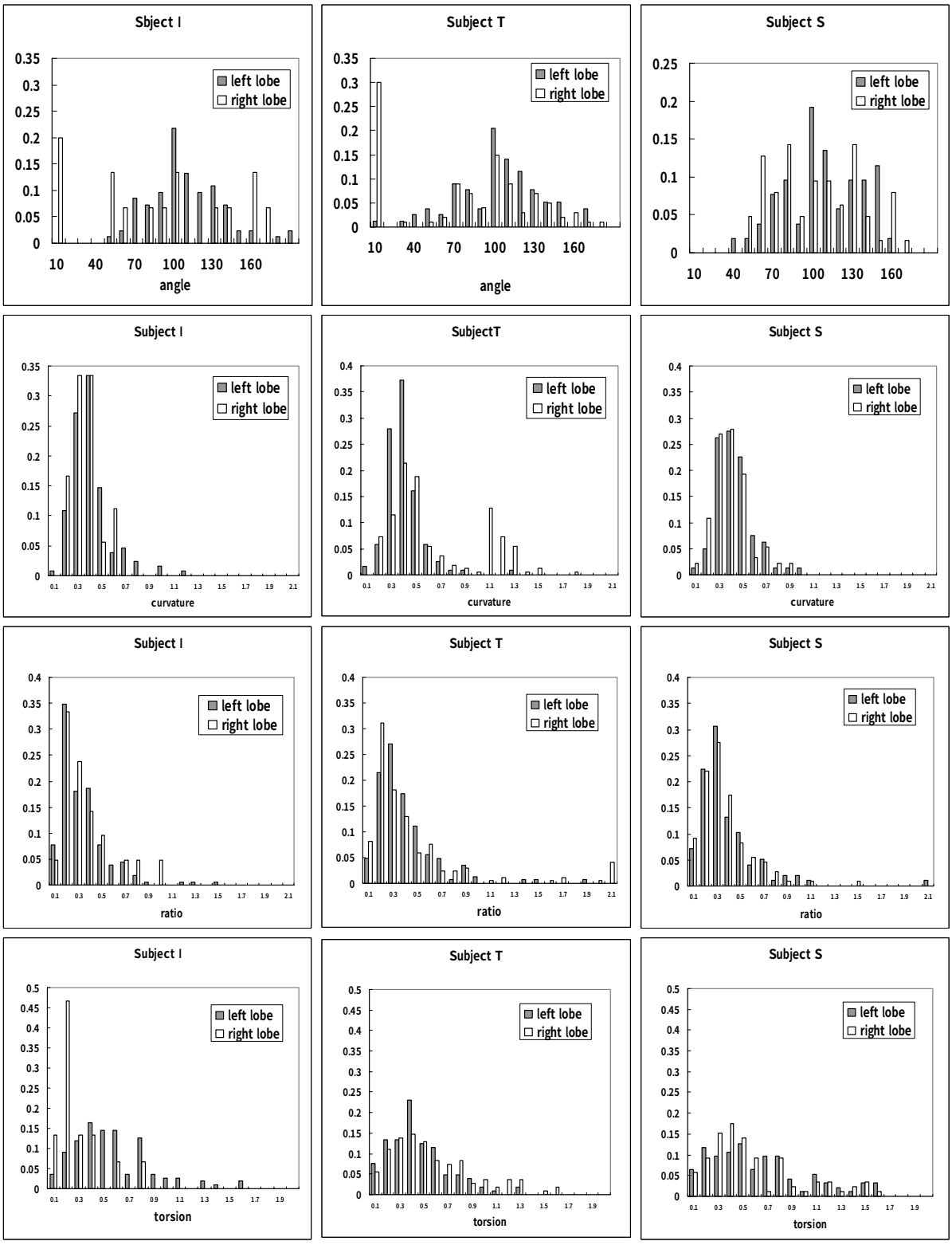

Figure.11- Results of the features calculated for each subject

branch angle and curvature for subject T and those for subject I and S, while the ratio distributions of all subjects are similar. The results of torsion may differ to each other, but the small number of calculation does not support the difference.

VII. Conclusion and future works

In this paper we proposed a method to extract four vascular features from liver images of CTAP of hepatic cirrhosis. The proposed method has been implemented and a three-dimensional shape of blood vessels in the liver from CT-images of three subjects were extracted, and the features proposed were calculated and shown for the right and left lobes of each subject. We will conduct more experiences in order to validate the proposed features with CT images in more higher and isotropic resolution. Also we plan future works including: use of the fractal dimensionality, extraction of the liver region, improvement of blood vessels, and more sophisticated thresholding and thinning procedure.

Acknowledgment

The authors would like to thank Professor Shinji Yamamoto of Chukyo University and Professor Sai Tokugi of Niigata University for their valuable suggestions, and colleagues, especially W. Yamaizumi and M. Hirano, Yamamoto Lab, Niigata University for helpful discussions and comments. This work was supported in part by the Center for Transdisciplinary Research (Prof. Miyakawa).

References

[1] S. Sherlock, J. Dooley, "Disease of the Liver and Biliary System," Blackwell Publishing Company, pp 315-328, 2002.

[2] S. Yamamoto, M.Matsumoto, Y. Tateno, T. Iinuma, T. Matsumoto, "Quoit Filter – A New Filter Based on Mathematical Morphology to Extract the Isolated Shadow, and Its Application to Automatic Detection of Lung Cancer in X-ray CT," Proceedings of the 13th International Conference Recognition, vol.2, pp 3-7, 1996.

[3] K. Furuishi, A. Frukawa, M, Takahashi, K. Murata, "Role of combined CT hepatic angiography and CT during arterial portography in the management of patients with hepatocellular carcinomas and liver metastases," Hepatology Research, vol.28, pp 191-197, 2004.

[4] Y.F.Tsao, K.S.Fu, "A parallel thinning algorithm for 3-D pictures," CGIP, vol.17, pp. 315-331, 1981.

[5] T. Saito, J. Toriwaki, "New algorithm for n-dimensional Euclidean distance transformation," Proc. of the 8th SCIA-93 (Scandinavian Conf. on Image Analysis), pp. 747-754, 1993.

[6] T. Saito, J.Toriwaki, "A sequential thinning algorithm for three dimensional digital pictures using the Euclidean distance transformation," Proc. 9th SCIA (Scandinavian Conf. on Image Analysis), pp. 507-516. 1995.

[7] T. Yoshikawa, et al, "Heterogeneity of Cerebral Blood Flow in Alzheimer Disease and Vascular Dementia," AJNR Am J Neuroradiol, vol.24, pp 1314-1347, August 2003.